



Nanosized Nickel doped Copper Chromite Spinel Particles: Synthesis, Characterization and Photocatalytic Applications

Prabhulkar S.G. and Patil R.M.

Department of Chemistry, The Institute of Science, 15, Madam Cama Road, Mumbai-400 032, INDIA

Available online at: www.isca.in, www.isca.me

Received 7th September 2012, revised 18th September 2013, accepted 14th October 2013

Abstract

Investigation of the nickel doped copper chromite spinel nanoparticles ($Ni_xCu_{1-x}Cr_2O_4$), where $x = 0.0, 0.2, 0.4, 0.6, 0.8, 1.0$) for the photocatalytic degradation of Thiazole Yellow G an azo dye indicator is studied in the present work. The nanoparticles were synthesized by simple, economic and ecofriendly coprecipitation method and were characterized by various physicochemical techniques such as X-ray diffraction analysis, Infra-red spectroscopy, Field Emission Gun – Scanning Electron Microscopy and Energy Dispersive Spectroscopy for the determination of crystallinity, metal-oxygen bonding, nanosized nature and elemental composition respectively. Various parameters affecting the photocatalytic dye degradation such as time, catalyst quantity and extent of doping were studied. This study provides clean and benign photocatalytic route for the degradation of the environmentally hazardous Thiazole Yellow G dye.

Keywords: A. Nanoparticles, B. Coprecipitation, C. XRD, D. IR, E. FEG-SEM, F. Photocatalysis.

Introduction

Though dyes are quite useful in day-to-day life of human race; the natural resources of water are being continuously polluted by various textile, dying and printing industries universally by the discharge of these dyes in their drainage system. Nearly 20% of the total world production of dyes is lost during the dyeing process. The dyes containing one or more azo bonds (-N=N-), called 'Azo dyes' are among the most widely used synthetic dyes and usually are the major pollutants that pollute natural waters. Azo dyes are a class of colored organic compounds that have largely used in industry for many applications such as textiles, papers, leathers, additives and indicators in analytical chemistry¹. During dye production and textile manufacturing process, and analytical laboratories a large quantity of wastewater containing dye stuffs with intensive color and toxicity are introduced into the aquatic systems². Many of the azo dyes have found to be highly toxic³ and mutagenic to aquatic flora and fauna⁴. The molecular structures of such azo dyes are found to be highly stable and are resistant to both chemical and biological degradation⁵⁻⁷. Therefore, these dyes are found to be highly hazardous to environment even at low concentrations. Inorganic solid state materials like Al_2O_3 doped with Cr^{3+} ions (Ruby laser), $Y_3Al_5O_{12}$ doped with Nd^{3+} ions and some semiconductor lasers like AlGaAs, InGaAs, InGaAsP have found various uses in photochemistry such as for the production of LASER⁸. Some co-doped (Ag, Co) ZnO nanoparticles have found to have antibacterial activity⁹. Photocatalytic oxidation (PCO) for the degradation of some azo dyes and other organic pollutants using TiO_2 as a photocatalyst has been reported in the literature¹⁰. Inorganic compounds such as mixed-metal oxide spinel nanoparticles have found to have

various applications as catalysts in various synthetic organic reactions¹¹.

The present work deals with the synthesis and characterization of the nickel substituted copper chromite spinel nanoparticles prepared by coprecipitation method and their applications to the photocatalytic degradation of catalytic reactions. Copper chromite spinel nanoparticles ($Ni_xCu_{1-x}Cr_2O_4$), where $x = 0.0, 0.2, 0.4, 0.6, 0.8, 1.0$) have not been used for the photocatalytic degradation of azo dye Thiazole Yellow G. The nanoparticles prepared were characterized by XRD analysis for their phase determination and crystallinity, IR spectrometry for the metal oxygen bonding, FEG-SEM for size determination and EDS for elemental composition. The present nanoparticles are easily dispersible but insoluble in water. These nanoparticles are selected to exploit their black colour for photocatalytic degradation of the selected Thiazole Yellow G (TYG) indicator as an azo dye.

Material and Methods

Material: The analytical reagent grade nickel nitrate [$Ni(NO_3)_2 \cdot 6H_2O$], copper nitrate [$Cu(NO_3)_2 \cdot 3H_2O$], Chromium nitrate [$Cr(NO_3)_3 \cdot 9H_2O$], Thiazole Yellow G (CDH), sodium hydroxide [NaOH] and hydrogen peroxide [H_2O_2] 30% (100 volumes); ($\geq 99\%$) were used as starting materials. Double distilled water was used throughout to prepare the solutions of metal nitrates and sodium hydroxide and washings of the filtered products.

Methods: Nanocrystalline powders of $Ni_xCu_{1-x}Cr_2O_4$ were prepared by co-precipitation method¹². The stoichiometric solutions of the metal salts were prepared and mixed slowly

with constant stirring. The pH of the solution was brought to and maintained between 9.0 and 9.5 by using 10% NaOH solution with the help of Equiptronics digital pH meter. The product obtained was digested on a boiling water bath for 3 hours and oxidized by 30% (100 volumes) hydrogen peroxide solution. The digested product was further aged by keeping overnight, filtered and washed several times with double distilled water and dried in hot air oven at 110°C. The compounds obtained were ground finely in agate mortar and pestle. The samples were investigated for optimization of the reaction temperature on Rigaku TG/DT Analyzer at heating rate of 10°C min⁻¹. The TG/DTA thermograms show no weight loss after 700°C and therefore, the present compounds were uniformly sintered in Eurocon automated programmable furnace at 750°C at the heating rate of 4°C per minute for 3 hours to get the crystalline single phase. The prepared samples have been designated as follows:

Sr. No.	Nanoparticle composition	Designation
1	Cu _{1.0} Ni _{0.0} Cr ₂ O ₄	CCr
2	Cu _{0.8} Ni _{0.2} Cr ₂ O ₄	CNCr-1
3	Cu _{0.6} Ni _{0.4} Cr ₂ O ₄	CNCr-2
4	Cu _{0.4} Ni _{0.6} Cr ₂ O ₄	CNCr-3
5	Cu _{0.2} Ni _{0.8} Cr ₂ O ₄	CNCr-4
6	Cu _{0.0} Ni _{1.0} Cr ₂ O ₄	NCr

Instrumental techniques: The prepared materials were characterized on 'Rigaku Miniflex II DESKTOP X-ray DIFFRACTOMETER' (Cu K α_1 radiation source with $\lambda = 1.5419 \text{ \AA}$) for the phase structure determinations. Infra-Red spectra of the samples were scanned on Perkin Elmer *precisely* Spectrum-100 FT-IR Spectrometer for the confirmation of the metal-oxygen bonds.

The series of Ni_xCu_{1-x}Cr₂O₄ particles were coated with Au-Pd plasma coating with the help of JEOL JFC-1600 Auto-fine coater and analyzed for their size determination in JEOL JSM-7600 F Field Emission Gun – Scanning Electron Microscope inbuilt with X-Max 80 mm² (Oxford instruments) Energy Dispersive X-ray Analyzer (EDS) for the study of elemental analysis.

The absorbance measurements of the dye solutions were made on Elico SL-150 UV-Vis spectrophotometer by using the quartz cuvette of pathlength 1cm².

Catalytic activity: The nanoparticles were used for their photo-catalytic activity towards the degradation of a toxic Thiazole Yellow G in the presence of 0.05g of catalyst in 15 Watts Bajaj CFL lamp with constant stirring at room temperature. The optimized reaction conditions were obtained by using nickel chromite as a model catalyst.

The progress of the reaction was monitored on UV-Visible Spectrophotometer for the deviation of absorbance at $\lambda_{max} = 405 \text{ nm}$ of the of the initial dye solution. Equal amounts of dye solutions were placed in four different beakers: i. First beaker containing azo dye solution – in dark. ii. Second beaker containing azo dye solution – in light. iii. Third beaker containing azo dye solution + 0.05 g NiCr₂O₄ nanoparticles – in dark and iv. Fourth beaker containing azo dye solution + 0.05 g NiCr₂O₄ nanoparticles – in light.

After completion of the reactions, the photo-catalyst nanoparticles were separated by magnetic separation and washed initially with warm double distilled water followed by acetone. The reactions were also carried out in absence of catalysts under optimized reaction conditions.

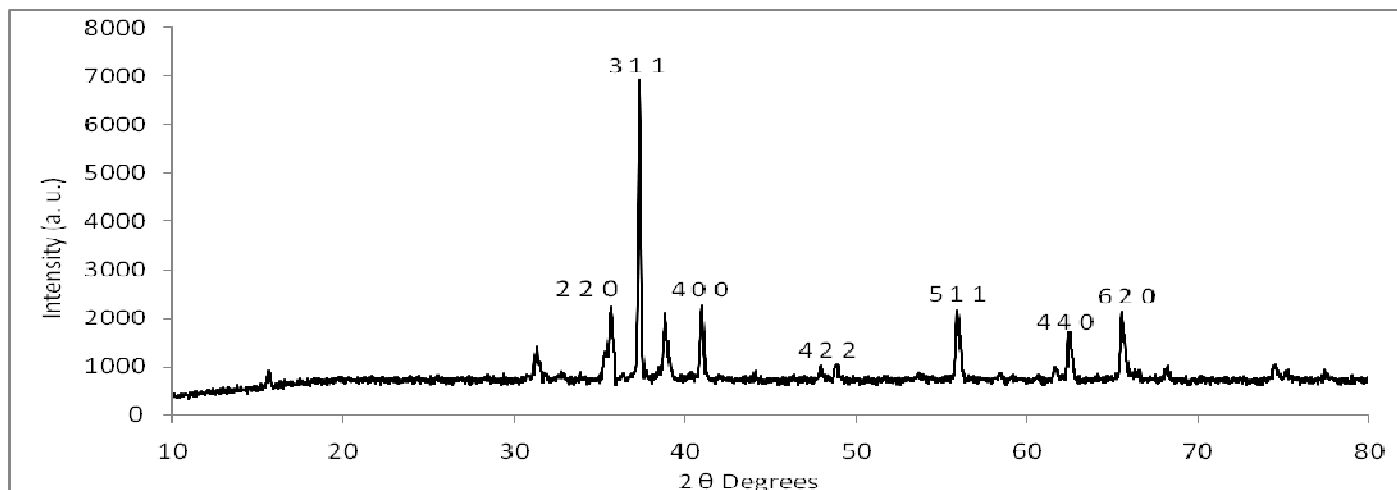
Results and Discussion

Thermal analysis: The TG curve results of all the samples have shown the weight loss of the samples up to the temperature ~700°C, after which all the samples evidently shown no further decrease in their weight content. Thus, the calcination temperature for all the compounds was optimized at the 750°C for all the samples to heat in an Eurocon automated programmable furnace at the rate of 4°C per minute for 3 hours.

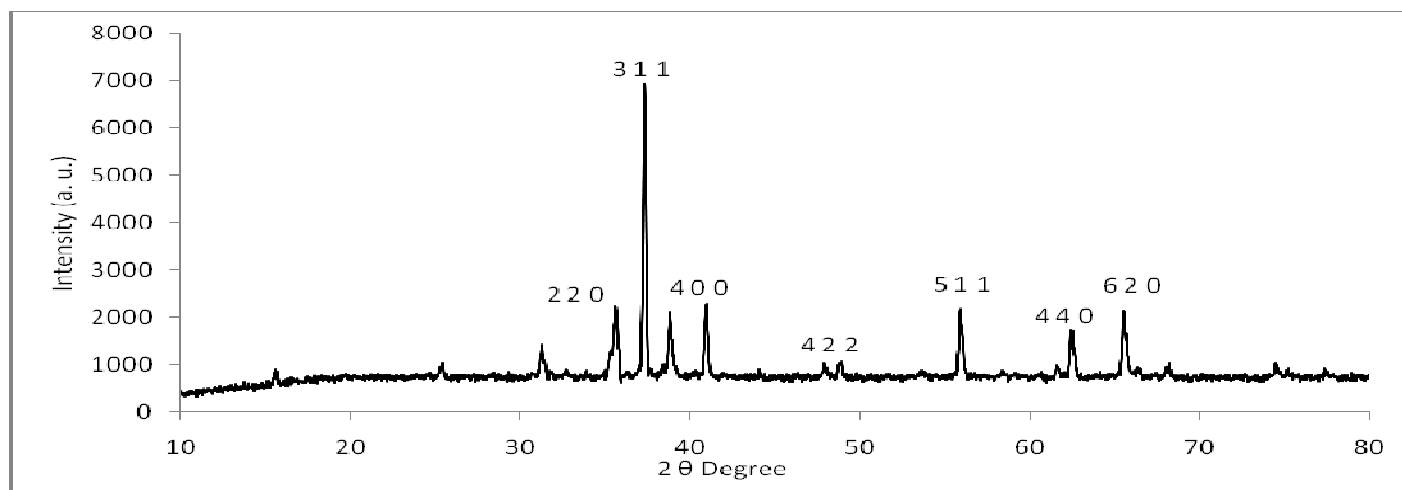
X-Ray diffraction studies: The literature survey reveals that the room temperature as is (without smoothing) X-ray diffraction patterns of samples sintered at the temperature of 750°C are in good agreement for the existence of single-phase spinel crystalline structures for all the samples as shown in figure- 1 (a) to (f). The theoretical and experimental d_{hkl} values for simple spinels are well coordinated^{13,14}. Indexing of X-ray diffraction patterns of most intense peaks are given in the table-1.

Table-1
Indexing of the X-ray diffraction patterns of peaks with $I/I_0 = 100 \%$

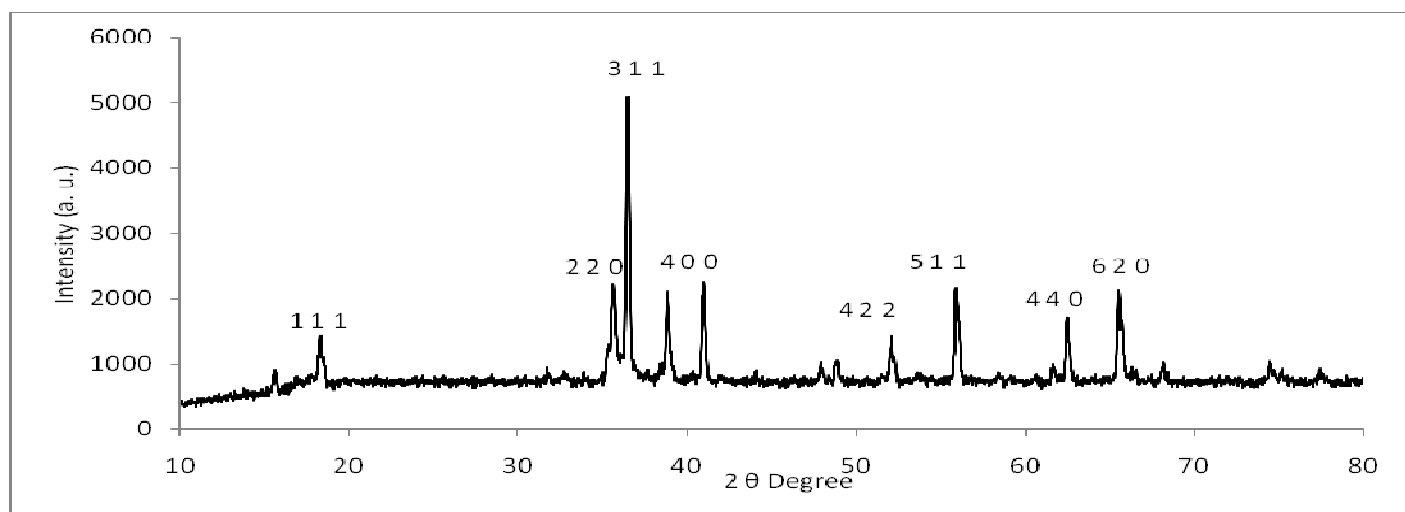
Sr. No.	Sample	2 θ Values	Intensity	d- Value
1	CCr	31.480°	6923	2.6613
2	CNCr – 1	31.580°	29923	2.8307
3	CNCr – 2	35.280°	2058	2.5419
4	CNCr – 3	35.360°	1755	2.5363
5	CNCr – 4	35.340°	2186	2.5377
6	NCr	35.900°	1784	2.4994



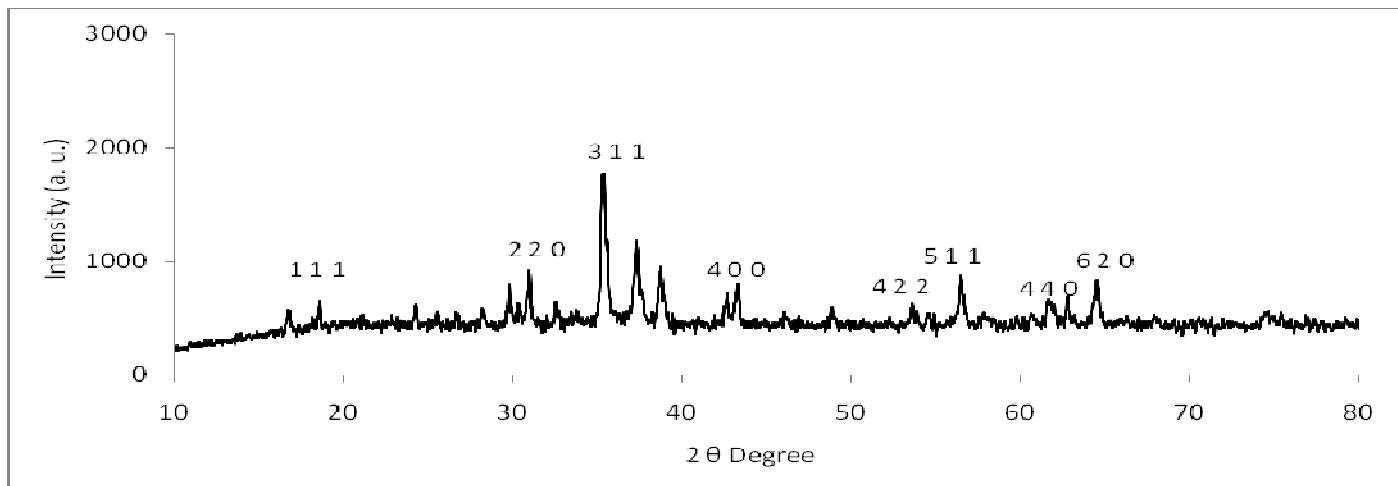
(a) XRD Pattern of CCr



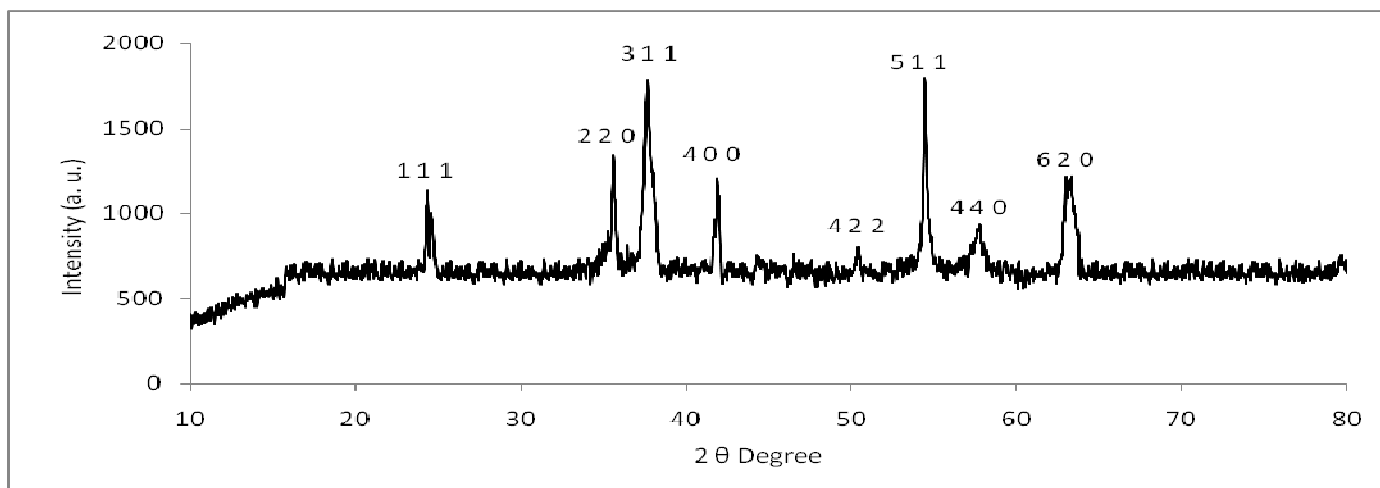
(b) XRD Pattern of CNCr - 1



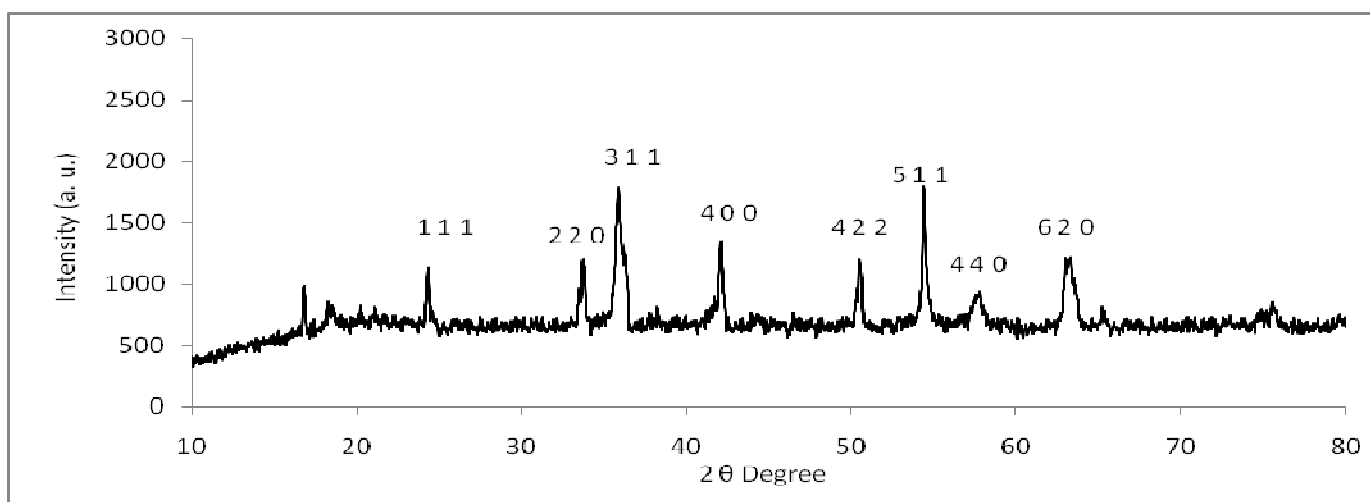
(c) XRD Pattern of CNCr-2



(d) XRD Pattern of CNCr - 3



(e) XRD Pattern of CNCr - 4



(f) XRD Pattern of NCr

Figure-1

X-ray diffraction patterns of the compounds CCr to NCr

Energy Dispersion Spectroscopy and Field Emission Gun-Scanning Electron Microscopy for particle size analysis:

The metal content stoichiometry of the compounds used for the preparation of the samples was taken as theoretical composition while the observed stoichiometry was calculated from EDS studies. The theoretical and calculated values of metal content stoichiometry are in good agreement with the chemical composition shown in table-2.

FT-IR studies: The FT-IR spectra of the samples in KBr powder were scanned. The vibrational frequencies depend on the cation mass, cation-oxygen bond length and the bond strength. The values of vibrational frequencies for tetrahedral (ν_1), octahedral (ν_2) sites and differences ($\nu_1 - \nu_2$) are given in the table-3.

The bands at higher and lower wavelength regions are assigned by Yu'eva et. al.¹⁵ to the vibrations of tetrahedral metal-oxygen bond (Ni-O and/or Cu-O) and octahedral metal-oxygen bond (Cr-O) respectively. A comparison of the

observed vibrational frequencies of all the compositions indicates that the ν_2 (corresponding to octahedral unit) remains almost unmodified. However, ν_1 (corresponding to tetrahedral unit) is observed to decrease smoothly with increase in Ni^{2+} content. The decrease in vibrational frequency (ν_1) with Ni^{2+} content can be attributed to the decreasing force constant and lengthening of M-O bonds of the tetrahedral unit. The Ni^{2+} preferably enters the tetrahedral site decreasing the force constant of Ni-O bond. This is also reflected in the $\nu_1 - \nu_2$ difference which decreases with increase in Ni^{2+} substitution.

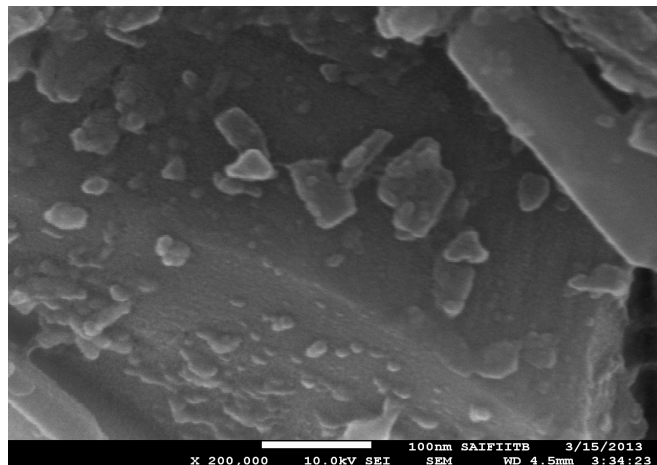
Size of the particles: The results of particle size for the series $Ni_xCu_{1-x}Cr_2O_4$ in JEOL JSM - 7600 F Field Emission Gun - Scanning Electron Microscope inbuilt with X-Max 80 mm² (Oxford instruments) Energy Dispersive X-ray Analyzer (EDS) are in the range of 11.9 to 63.3 nm can be termed as 'Nanoparticles' throughout¹⁶. FEG-SEM images and the histogram showing the size of the prepared nanoparticles are shown in figure- 2 (a) to (f) and Figure- 3 respectively.

Table-2
Elemental composition by EDS and particle size of the nanoparticles from FEG-SEM

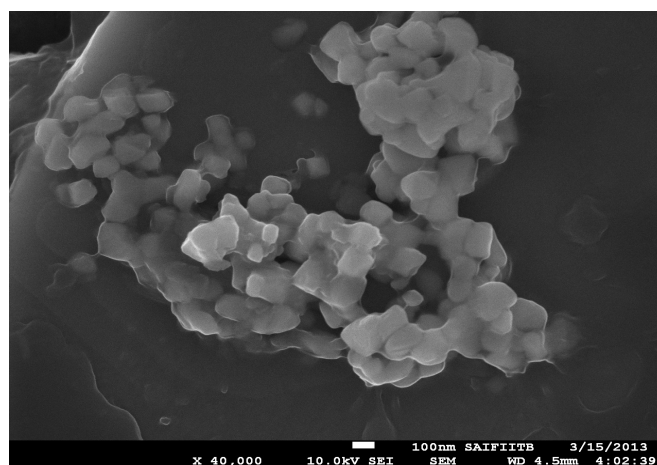
Sample	Atom percentage (Theoretical)				Atom percentage by EDS				Particle size (nm)
	Cu	Ni	Cr	O	Cu	Ni	Cr	O	
CCr	27.45	00.00	22.46	50.09	26.84	00.00	23.03	50.13	16.9
CNCr-1	22.05	05.09	45.10	27.76	21.73	05.16	45.53	27.58	63.3
CNCr-2	16.61	10.23	45.29	27.87	16.72	10.11	45.27	27.90	30.9
CNCr-3	11.12	15.40	45.49	27.99	11.48	15.33	45.24	27.95	30.1
CNCr-4	05.58	20.63	45.68	28.11	05.69	20.59	45.67	28.05	30.0
NCr	00.00	25.89	45.88	28.23	00.00	25.80	46.00	28.20	11.9

Table-3
Values of vibrational frequencies for tetrahedral (ν_1), octahedral sites (ν_2)

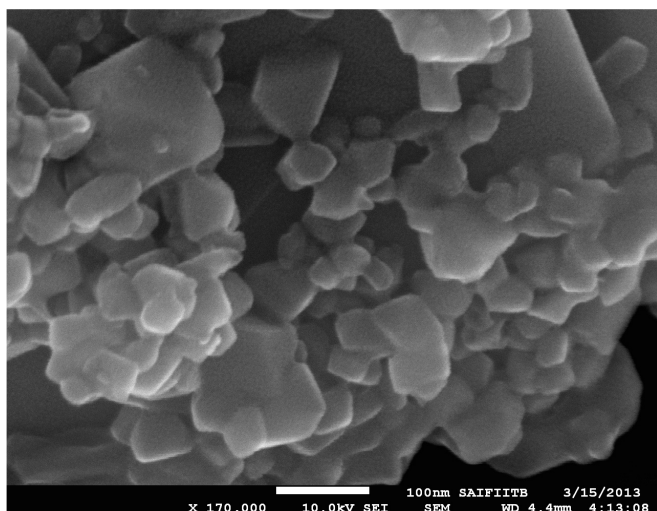
Sr. No.	Nanoparticle	ν_1 cm ⁻¹ (Td)	ν_2 cm ⁻¹ (Oh)	$\nu_1 - \nu_2$ cm ⁻¹
1	CCr	571	426	145
2	CNCr-1	561	427	134
3	CNCr-2	558	428	130
4	CNCr-3	549	430	119
5	CNCr-4	542	432	110
6	NCr	536	435	101



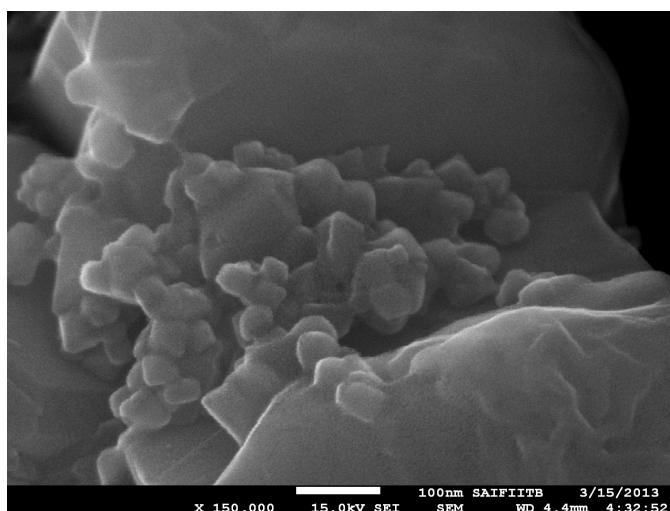
(a). FEG-SEM image of CCr



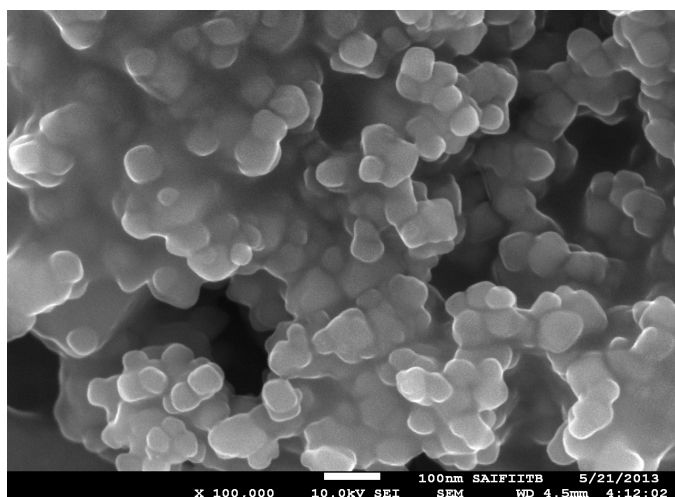
(b). FEG-SEM image of CNCr-1



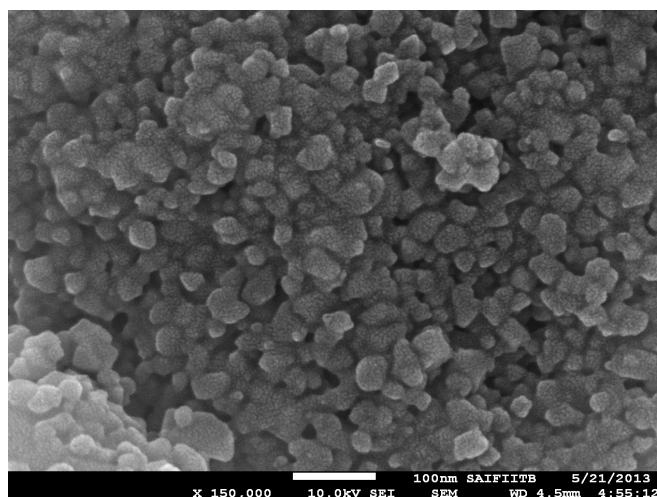
(c). FEG-SEM image of CNCr-2



(d). FEG-SEM image of CNCr-3



(e). FEG-SEM image of CNCr-4



(f). FEG-SEM image of NCr

Figure-2

Field Emission Gun–Scanning Electron Microscopic images of the compounds CCr to NCr on Carbon base and Au-Pd sputtering

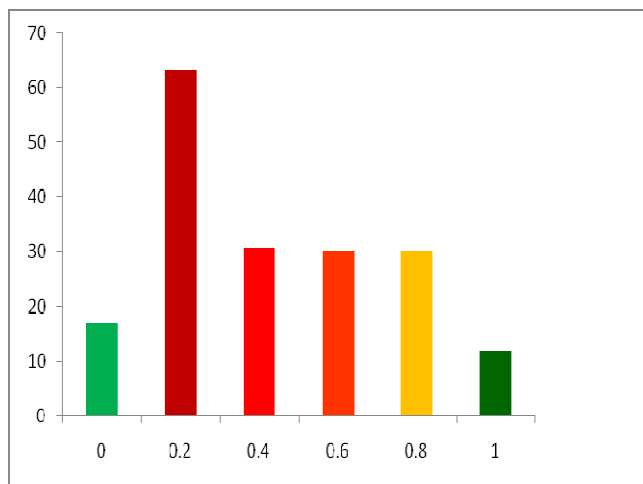


Figure-3

Histogram of the size of the nanoparticles of the system $Ni_xCu_{1-x}Cr_2O_4$

Catalytic performance: The materials thus characterized for structure, composition and particle sizes were then used as catalysts to evaluate their photocatalytic efficiency for degradation of Thiazole Yellow G dye.

Photo catalytic activity of $NiCr_2O_4$ as a function of time: A plot of absorbance of Thiazole Yellow G solution (100 ppm) at λ_{max} of 405 nm after catalyst equilibrations at various time intervals of constant stirring is plotted in figure- 4 and the absorbance values of the aliquots for different time intervals are tabulated in table-4.

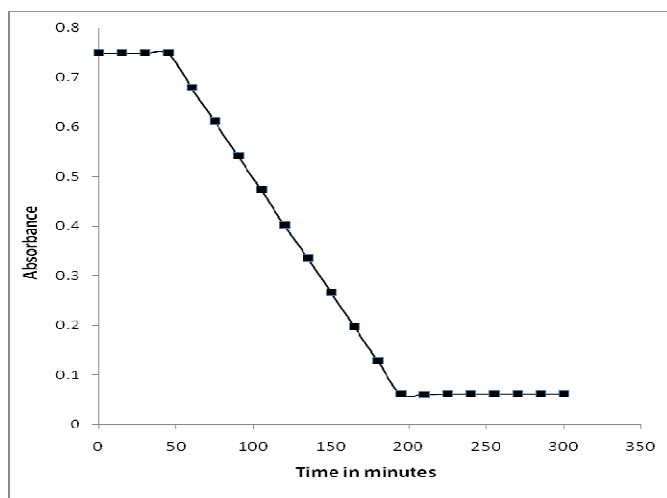


Figure-4

Photo catalytic activity of $NiCr_2O_4$ as a function of time

The plot shows that the degradation of 100 ppm of TYG, photo-catalyzed by $NiCr_2O_4$ was started at the time of 45 minutes of constant stirring under the light radiation. The degradation of the 100ppm dye solution showed a linear decrease in the absorbance till 210 minutes after which there was no significant

decrease in the absorbance of the solution. Hence, the equilibration time required for complete photodegradation of TYG was found to be 210 minutes.

Table-4

Photo catalytic activity of $NiCr_2O_4$ as a function of time

Sr. No.	Time	Absorbance
1	00	0.749
2	15	0.749
3	30	0.749
4	45	0.749
5	60	0.700
6	75	0.680
7	90	0.611
8	105	0.542
9	120	0.473
10	135	0.404
11	150	0.335
12	165	0.266
13	180	0.197
14	195	0.129
15	210	0.059
16	225	0.059
17	240	0.059
18	255	0.059

Effect of amount of NCr nanoparticles on the of azo-dye degradation: The optimum quantity of the photocatalyst was determined by varying the amount of catalyst and carrying out the photodegradation of the catalyst for 210 minutes. Absorbances of the aliquots were recorded for Equilibration time of 210 minutes at λ_{max} of 405 nm. The results obtained show that, the optimum quantity of 0.050 g was required for the photocatalytic degradation of TYG. The results are plotted in figure- 5 and tabulated in table-5.

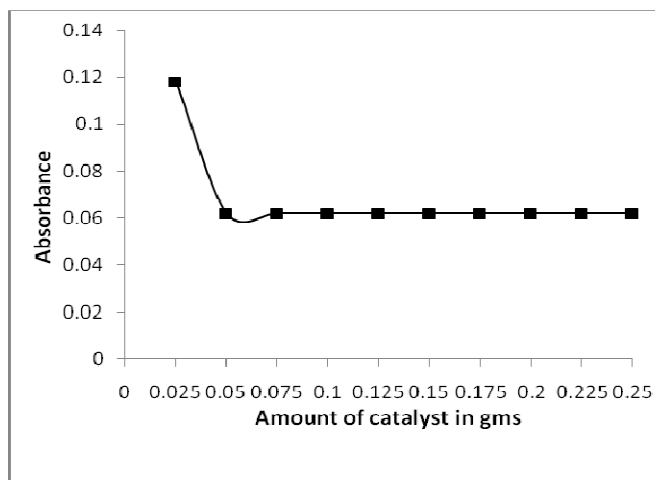


Figure-5

Effect of amount of NCr nanoparticles on the of azo-dye degradation

Table-5
Effect of amount of NCr nanoparticles on the of azo-dye degradation

Sr. No.	Amount of catalyst in gms	Absorbance
1	0.025	0.118
2	0.050	0.059
3	0.075	0.059
4	0.100	0.059
5	0.125	0.059
6	0.150	0.059
7	0.175	0.059
8	0.200	0.059

Catalyst selectivity: A series of photocatalytic nanoparticles of $Ni_xCu_{1-x}Cr_2O_4$ were investigated for the better selectivity of the degradation of TYG. It was found that, $NiCr_2O_4$ gives better selectivity for the photocatalytic degradation of the TYG dye. The results obtained for catalyst selectivity with [Catalyst] = 0.050 gms, [TYG] = 100 ppm, Equilibration time = 210 minutes are tabulated in Table-6.

Table-6
Catalyst selectivity

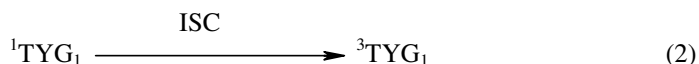
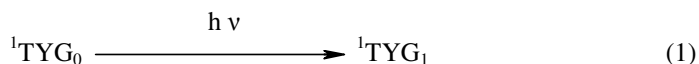
Sr. No.	Nanoparticle	Absorbance
1	CCr	0.062
2	CNCr-1	0.269
3	CNCr-2	0.185
4	CNCr-3	0.170
5	CNCr-4	0.164
6	NCr	0.058

Catalyst reusability: The reusability of the selected 0.050 gms $NiCr_2O_4$ nanoparticles catalyst was separated from the aliquots after every 210 minutes, by magnetic separation and washed with hot double distilled water followed by acetone. The catalyst was annealed at 110°C and reused for the photocatalytic degradation for further six cycles which shows negligible reduction in the catalyst activity at the sixth cycle. The results are tabulated in Table-7

Table-7
Catalyst reusability

Sr. No.	No. of Cycles	Absorbance
1	1	0.058
2	2	0.058
3	3	0.058
4	4	0.059
5	5	0.059
6	6	0.061

Reaction Mechanism: These observations lead to a tentative mechanism for the photocatalytic degradation of Thiazole Yellow G as follows:



The radiations of suitable wavelength are absorbed by Thiazole Yellow G (1TYG_0) which leads to generation of its excited singlet state (1TYG_1). This excited singlet state undergoes intersystem crossing (ISC) and gives the triplet state (3TYG_1) of TYG. Whilst the $Ni_xCu_{1-x}Cr_2O_4$ nanoparticles, absorb the light energy to excite its electron (e^-) from valence band (VB) to the conduction band (CB) of spinel nanoparticles (SP); and a hole (h^+) is created in valence band. This hole in the valence band of semiconducting nanoparticles oxidize the dye molecules to its leuco form (TYG^+) and as a consequence, decomposition of the dye results to the bleaching of TYG dye.

Conclusion

From the results obtained we conclude that nanosized nickel doped copper chromite spinel particle catalysts obtained by the safest, economic, convenient and eco-friendly coprecipitation method provides an interesting benign photocatalytic route for the degradation of Thiazole Yellow G. The $NiCr_2O_4$ nanoparticles show better activity among all the compounds investigated for the successful photodegradation of TYG. This study reveals that the prepared nickel chromite spinel nanoparticles are the convenient and eco-friendly substitutes over the hazardous stoichiometric reagents, bleaching agents and can be used in effluent treatment of the dyes, pigments in the industries.

References

1. Dakiky M. and Nemcova I., *J.Dyes Pigments*, **44**, 181 (2000)
2. Brown M.A. and De Vito S.C., *J.Environ. Technol.*, **23**, 249 (1993)
3. Meyer U., Biodegradation of synthetic organic colorants. In: Leisinger T., Cook, A.M., Naesch J. and Haffer, R. (Eds.), *Microbial Degradation of Xenobiotics and*

- Recalcitrant Compounds*. Academic Press, London, UK, pp. 389–399 (1981)
4. Chung K.T., Fulk G.E. and Andres A.W., Mutagenicity testing of some commonly used dyes. *Applied and Environmental Microbiology*, **42**, 641–648 (1981)
 5. Dai S., Zhuang Y., Chen Y. and Chen L., Study on the relationship between structure of synthetic organic chemicals and their biodegradability, *Environmental Chemistry*, **14**, 354–367 (1995)
 6. Dai S., Song W., Li T. and Zhuang Y., Study on azo dyes structure – biodegradability relationships, *Advances in Environmental Sciences*, **4**, 1–9 (1996a)
 7. Dai S., Song W., Zhuang Y. and Yan H., Biotechnical treatment of wastewater containing azo dyes, In: Proceedings of the 4th Mainland–Taiwan Environmental Technology Seminar, **1**, 407–411 (1996b)
 8. Rao M.C., *Res. J. Mat. Sci.*, **1(2)**, 20 (2013)
 9. Reddy S.B., Reddy V.S., Reddy K.N. and Kumari P.J., *Res. J. Mat. Sci.*, **1(1)**, 11 (2013)
 10. Tanaka K., Padermpole K. and Hisanaga T., Photocatalytic degradation of commercial azo dyes, *Water Research*, **34**, 327–333 (2000)
 11. Prabhulkar S.G. and Patil R.M., *Res. J. Mat. Sci.*, **1(4)**, 18 (2013)
 12. Dube G.R. and Darshane V.S., *Bull. Chem. Soc. Jpn.*, **64**, 2449 (1991)
 13. X-ray Powder Data File JCPDS, Philadelphia, PA, , 21-874 (1973)
 14. George K. and Sugunan S., *Cat. Comm.*, **9**, 2149, (2008)
 15. Yur'eva T.M., Boreskov G.K., Zharkov V.I., Karakchivev L.G., Popovski V.V. and Chigrina V., A., *Kinet. Katal.*, **9**, 1063, (1968)
 16. Charles P. Poole, Jr. and Frank J. Owens, Introduction to Nanotechnology, John Wiley and Sons, (2003)